British Journal of Pharmacology

British Journal of Pharmacology (2018) **175** 2611–2621 2611

RESEARCH PAPER

Treatment with IL-19 improves locomotor functional recovery after contusion trauma to the spinal cord

Correspondence Shuxun Hou, Department of Orthopaedics, First Affiliated Hospital of Chinese People's Liberation Army General Hospital, 51 Fucheng Road, Beijing 100048, China. E-mail: houshuxun2012@hotmail.com

Received 28 March 2017; **Revised** 7 February 2018; **Accepted** 8 February 2018

Jidong Guo*, Huadong Wang*, Li Li*, Yanli Yuan, Xiuxiu Shi and Shuxun Hou

Institute of Orthopaedics, First Affiliated Hospital of CPLA General Hospital, Beijing, China

*The first three authors contributed equally to the work.

BACKGROUND AND PURPOSE

IL-19 skews the immune response towards a Th2 type and appears to stimulate angiogenesis. In the current study, we tested if IL-19 treatment could reduce secondary injury and improve functional recovery after contusion spinal cord injury (SCI).

EXPERIMENTAL APPROACH

Firstly, mice were given a moderate–severe thoracic SCI at the T_{9-10} level and expression of IL-19 and its receptor was measured in the injured spinal cord. Then SCI mice were treated with mouse recombinant IL-19 and its blocking antibody to investigate the therapeutic effect of IL-19.

KEY RESULTS

Protein expression of IL-19 and its receptor IL-20R1 and IL-20R2 was up-regulated in the injured spinal cord of mice. IL-19 treatment promoted the recovery of locomotor function dose-dependently and reduced loss of motor neurons and microglial and glial activation following SCI. Treatment of SCI mice with IL-19 attenuated macrophage accumulation, reduced protein levels of TNF-α and CCL2 and promoted Th2 response and M2 macrophage activation in the injured region. Treatment of SCI mice with IL-19 promoted angiogenesis through up-regulating VEGF in the injured region. Treatment of SCI mice with IL-19 up-regulated HO-1 expression and decreased oxidative stress in the injured region. The beneficial effect of IL-19 was abolished by coadministration of the blocking antibody. Additionally, IL-19 deficiency in mice delayed the recovery of locomotor function following SCI.

CONCLUSIONS AND IMPLICATIONS

IL-19 treatment reduced secondary injuries and improved locomotor functional recovery after contusion SCI, through diverse mechanisms including immune cell polarization, angiogenesis and anti-oxidative responses.

Abbreviations

BMS, Basso Mouse Scale; GFAP, glial fibrillary acidic protein; HO-1, haem oxygenase 1; IBA1, ionized calcium-binding adapter molecule 1; MDA, malondialdehyde; PECAM-1, platelet endothelial cell adhesion molecule-1; SCI, spinal cord injury

DOI:10.1111/bph.14193

Introduction

Spinal cord injury (SCI), resulting in long-term and severe disability, influences the quality of life and triggers serious socio-economic consequences (McDonald and Sadowsky, 2002). Multiple cascades of pathophysiological processes rapidly follow the primary injury (the initial mechanical trauma to spinal cord), leading to secondary neuronal damage that causes further dysfunction (Oyinbo, 2011). The detrimental secondary events develop minutes to weeks after SCI, including loss of motor neurons, gliosis, inflammation and oxidative stress (Jia *et al.*, 2012; Ren and Young, 2013). It is known that effective restraint of secondary injury is important for minimizing loss of motor neurons and improving functional recovery following SCI.

The cytokine **IL-19**, as a unique Th2 interleukin first described in 2000, was originally placed in the IL-10 subfamily, which included IL-10, IL-19, **IL-20**, IL-22, IL-24, IL-26, IL-28 and IL-29. IL-19 shared 20% amino acid similarity with IL-10 but is functionally distinct from these sub-family members and especially IL-10 (Gallagher *et al.*, 2000; Sabat *et al.*, 2007). IL-19 signalled through a heterodimeric receptor composed of **IL-20R1** and **IL-20R2**, which was also utilized by IL-20 and IL-24 (Dumoutier *et al.*, 2001). IL-19 reduced inflammation in TNBS-induced experimental colitis (Matsuo *et al.*, 2015) and halted progression of experimental atherosclerosis (Ellison *et al.*, 2013; Gabunia *et al.*, 2016). More importantly, it was reported that IL-19 treatment reduced brain infarction and alleviated neurological deficits in a mouse model of cerebral ischaemia (Xie *et al.*, 2016). In the CNS, IL-19 was an anti-inflammatory cytokine, produced by activated microglia, which acted negatively on microglia in an autocrine manner (Horiuchi *et al.*, 2015). In our work, we found that IL-19 and its receptor were up-regulated in the spinal cord of mice after injury. We hypothesized that IL-19 may be beneficial for locomotor functional recovery after SCI, and we tested effect of mouse recombinant IL-19 and investigated the underlying mechanism(s) in a mouse model of SCI.

Methods

Animals and study design

All animal care and experimental procedures complied with the Animals (Scientific Procedures) Act, 1986 of the UK Parliament, Directive 2010/63/EU of the European Parliament and the Guide for the Care and Use of Laboratory Animals published by the US National Institutes of Health (NIH Publication No. 85–23, revised 1996) and were approved by the Animal Ethical Committee of the Chinese People's Liberation Army General Hospital. Animal studies are reported in compliance with the ARRIVE guidelines (Kilkenny *et al.*, 2010; McGrath and Lilley, 2015). IL-19 knockout mice were generated using the VelociGene method and identified by genotyping of tail DNA by PCR using specific primers as described earlier (Ellison *et al.*, 2014). All animals were on a C57BL/6 background, bred and housed under specific pathogen-free conditions.

Experiment 1: Mice (male, 20–25 g, n = 11 in each group) were randomly divided into two groups as follows: sham-operated group and SCI group. Seven days post-injury, protein (n = 3 for Western blotting analysis) and mRNA expression (n = 8 for RT-PCR analysis) of IL-19, IL-20R1 and IL-20R2 was assayed in the peri-lesional tissues (5 mm length of the spinal cord centred at the injury site or equivalent area in sham-operated mice).

Experiment 2: Male C57BL/6 mice (20–25 g) were exposed to spinal cord trauma and treated i.p. with IL-19 (5 and 10 $ng \cdot g^{-1}$ body $weight \cdot day^{-1}$, n = 7 in each group) (Ellison *et al.*, 2013; Xie *et al.*, 2016) or not. We used mouse recombinant IL-19, supplied by R&D Inc (Minneapolis, MN), diluted in 0.0025% BSA in sterile PBS. Locomotor function was monitored each day for 2 weeks.

Experiment 3: Male C57BL/6 mice (20-25 g) were randomly divided into three groups as follows: (i) SCI mice treated with vehicle; (ii) SCI mice treated with IL-19 (10 $ng \cdot g^{-1}$ body $weight \cdot day^{-1}$, i.p.); and (iii) SCI mice treated with IL-19 (10 $ng \cdot g^{-1}$ body $weight \cdot day^{-1}$, i.p.) and its blocking antibody (10 $mg \cdot kg^{-1} \cdot day^{-1}$, s.c.) (Hsu *et al.*, 2012). Locomotor function was monitored each day for 2 weeks (n = 7 in each group). Seven days post-injury, the mice were killed, and peri-lesional tissues were removed for several biochemical analyses (n = 7 for RT-PCR, n = 7 for immunofluorescence staining, n = 3 for Western blotting, n = 7 for measurement of malondialdehyde (MDA) and pro-inflammatory cytokines levels). Before injection i.p., mouse recombinant IL-19 was diluted in 0.0025% BSA in sterile PBS. Mouse recombinant IL-19 was used to generate anti-mIL-19 mAb (Monoclonal Rat IgG2B Clone 9C), according to standard protocols in our lab. The isotype of the selected antibody, IgG, was determined using an isotyping ELISA. The antibody was purified using protein A chromatography. The antibody was shown to have <0.5 $EU \cdot mg^{-1}$ endotoxin and be of >95% purity. Initial treatment was given 6 h after the trauma.

Experiment 4: Wild-type mice and IL-19(−/−) mice (male, 20–25 g, n = 6 in each group) were given SCI, and locomotor function was monitored each day for 2 weeks.

Mouse model of spinal cord trauma

Mice received a mid-thoracic spinal contusion trauma as described in Jakeman *et al.* (2000). Briefly, after the mice were fully anaesthetized (5% isoflurane in 30% O_2/70% N_2O), a partial vertebral laminectomy was performed at the mid-thoracic level (T9–10). The exposed dorsal spinal surface (T9 spinal level) was displaced a calibrated vertical distance (0.5 mm over ~25 ms), to produce a moderate contusion SCI using the Infinite Horizons Impactor (60 kdyn; Precision Systems and Instrumentation, Fairfax Station, VA, USA). During the surgery, the mice were placed on a controlled heating pad to maintain temperature at 37 ± 1°C. After the surgery, the mice were hydrated with physiological saline (2 mL, s.c.). Their bladders were manually expressed twice daily, and hydration was monitored daily. Analgesia was provided with buprenorphine (0.1 $mg \cdot kg^{-1}$; Temgesic, Schering-Plough, Belgium) injected s,c, 30 min before surgery and then the same dose every 12 h for 3 days. Mice that underwent laminectomy only served as sham controls.

Assessment of locomotor function

Hindlimb motor function was evaluated using the Basso Mouse Scale (BMS) open field locomotor test by two raters blinded to the study design (Basso *et al.*, 2006). The BMS is a 10-point locomotor rating scale, in which the scores range from 0 (complete hindlimb paralysis) to 9 (normal locomotion) points and include the assessment of ankle movement, plantar placement, weight support, stepping, coordination, paw position and trunk stability. Each mouse was observed separately for 4 min per session, and BMS scores were recorded. The mice with a BMS score higher than 0 at 24 h after injury were excluded from future evaluation.

Quantitative RT-PCR

Samples of spinal cords and spleens were homogenized in Trizol reagent (Life Technologies, Carlsbad, CA), and total RNA was isolated in accordance with the manufacturer's instructions. The purity of total RNA was measured with a Nanodrop 1000 spectrophotome-212-ter (Thermo Fisher Scientific, Waltham, MA), and the wavelength absorption ratio (260/280) was between 1.8 and 2.0 for all preparations. Reverse transcription was carried out with 1 μg total RNA using the Superscript First-Strand Synthesis System for RT-PCR (Invitrogen), and RT-PCR was performed with a QuantiTectTM SYBR® Green PCR (TIANGEN BIOTECH, Beijing, China). Samples were analysed in triplicate, and expression of GAPDH mRNA was used as reference gene to normalize data, and then the final results were related to the calibrator samples (sham-operated group or vehicle-treated group) using the formula $2^{-\Delta\Delta Ct}$. The sequences of primers were listed in Table 1.

Western blotting analysis

Proteins from peri-lesional tissues were extracted using RIPA (PBS containing 1% IGEPAL CA-630, 0.5% sodium deoxycholate, 0.1% SDS, 0.5 mM PMSF, 500 ng/mL Leupeptin, 1 μg/mL aprotinin, 2.5 μg/mL pepstatin A). The primary antibodies used were anti-IL-19 (Abcam, Cambridge, UK), anti-IL-20R1 (Abcam), anti-IL-20R2 (Abcam), anti-platelet endothelial cell adhesion molecule-1 (anti-PECAM-1) (Abcam), anti-**VEGF**-A (Abcam) and anti-**haem oxygenase 1** (anti-**HO-1**) (Abcam). Subsequently, the Western blot membranes were incubated with a HRP-coupled secondary antibody (GE Healthcare). Visualization was achieved by applying Supersignal West Pico- (Thermo Scientific) chemiluminescence HRP substrate, and band intensity was quantified by using the software Quantity One (version 4.5.2; Bio-Rad).

Immunofluorescence

Peri-lesional tissue sections (8 μm), taken from mice killed 7 days post-SCI, were used for immunofluorescence studies with antibodies specific for glial fibrillary acidic protein (GFAP) (Abcam), ionized calcium-binding adapter molecule 1 (IBA1) (Abcam), NeuN (Cell Signalling Technology) and CD68 (Abcam). Six sections per animal were analysed. Representative images of each sample were acquired by using a fluorescence microscope (Leica DM5500B with digital camera Leica DFC345 FX, Leica Microsystems, Germany) for immunolabelling quantification. Quantification of GFAP, Iba-1 and CD68 expression was performed by intensity analysis using ImageJ open source software (NIH) within rectangular areas of 100 μm × 100 μm.

Measurement of pro-inflammatory cytokines and VEGF-A

The peri-lesional tissues were homogenized in ice-cold RIPA containing 1% phenylmethanesulfonyl fluoride (Beyotime Institute of Biotechnology, Shanghai, China). The protein concentration was determined using Bradford dye-binding method (Beyotime Institute of Biotechnology). **TNF-α,** the chemokine **CCL2** and **VEGF-A** levels in peri-lesional tissues were determined by using ELISA kits (TNF-α and VEGF-A, R&D Systems, Minneapolis, MN, USA; CCL2, Thermo Fisher Scientific).

Lipid peroxidation determination

MDA, an intermediate product of lipid peroxidation, was determined by the thiobarbituric acid method with a kit (Cayman, Ann Arbor, MI, USA). Protein quantification was used for data normalization.

Data and statistical analysis

The data and statistical analysis comply with the recommendations on experimental design and analysis in pharmacology (Curtis *et al.*, 2015). In the current study, data are shown as the means ± SD. The data except BBB scores were analysed by one-way ANOVA followed by a *post hoc* Tukey test to compare the control and treatment groups. Comparison of BBB scores among groups was analysed using a two-way ANOVA followed by Bonferroni *t*-test. Following the ANOVA, *post hoc* tests were run only if F achieved the necessary level of statistical significance ($P < 0.05$) and there was no significant variance in homogeneity. Statistical significance was accepted for $P < 0.05$. Statistical analysis was performed using GraphPad Prism 5.0 (GraphPad Software, La Jolla, CA).

Nomenclature of targets and ligands

Key protein targets and ligands in this article are hyperlinked to corresponding entries in http://www.guidetopharmacology.org, the common portal for data from the IUPHAR/BPS Guide to PHARMACOLOGY (Harding *et al.*, 2018), and are permanently archived in the Concise Guide to PHARMACOLOGY 2017/2018 (Alexander *et al.*, 2017a,b).

Results

Expression of IL-19 and its receptor (experiment one)

To elucidate the role of IL-19 in SCI, we first examined whether the injury affected the expression of IL-19 and its receptor in the spinal cord. Seven days after spinal cord trauma, the mRNA (Figure 1A) and protein (Figure 1B) of IL-19 and its receptor IL-20R1 and IL-20R2 were higher in the injured spinal cord than that in sham-operated mice.

Table 1

Sequences of oligonucleotides used as primers

Target gene		Sequence (5′-3′)
IL-19	Sense	ATGACCAACAACC TGCTGACATTC
	Antisense	CAGTTCTCCTAG AGACTTAAGGG
IL-20R1	Sense	CTAAGTCGAGA AGAACGTGGT
	Antisense	TGACTTTAGCCT TCCATGCTGA
IL-20R2	Sense	GTGCACCTAGA AACCATGGA
	Antisense	CCATCTTCC AGACGGAGAG
NeuN	Sense	GGCAATGGT GGGACTCAAAA
	Antisense	GGGACCCGC TCCTTCAAC3
GFAP	Sense	CCAGCTTCG AGCCAAGGA
	Antisense	GAAGCTCCG CCTGGTAGACA
IBA1	Sense	GAGGAGCCAT GAGCCAAAGCA
	Antisense	CGAGGAATTG CTTGTTGATCCCC
IFN-γ	Sense	TGCGGGGTTG TATCTGGGGGT
	Antisense	GCGCTGGCCC GGAGTGTAGA
IL-12	Sense	GAGGAGAGTCT GCCCATTGAGGTC
	Antisense	GGGTGGGTCAG GTTTGATGATGTC
CD206	Sense	TCTTTGCCTT TCCCAGTCTCC
	Antisense	TGACACCCA GCGGAATTTC
Arg1	Sense	AAGAATGGAAG AGTCAGTGTGG
	Antisense	GGGAGTGTTG ATGTCAGTGTG
Ym1	Sense	AGAGTGCTGA TCTCAATGTGG
	Antisense	GGGCACCAA TTCCAGTCTTAG
iNOS	Sense	TTGGAGCGAG TTGTGGATTGT
	Antisense	GTAGGTGAGG GCTTGGCTGA
T-bet	Sense	TCAACCAGCA CCAGACAGAG
	Antisense	AACATCCTGTA ATGGCTTGTG

continues

Table 1

(Continued)

Target gene		Sequence (5′-3′)
GATA3	Sense	CTTATCAAGCCC AAGCGAAG
	Antisense	CCCATTAGCGT TCCTCCTC
$VEGF_{120}$	Sense	GTAACGATGAAG CCCTGGAG
	Antisense	CCTTGGCTTGT CACATTTTTC
$VEGF_{164}$	Sense	AGCCAGAAAATC ACTGTGAGC
	Antisense	GCCTTGGCTTG TCACATCT
$VEGF_{188}$	Sense	AGTTCGAGGAA AGGGAAAGG
	Antisense	GCCTTGGCTTG TCACATCT
HO-1	Sense	TCAGGTGTCCA GAGAAGGCTTT
	Antisense	CTCTTCCAGGGC CGTGTAGA
GAPDH	Sense	GCAAGGACACT GAGCAAGAG
	Antisense	GGGTCTGGGA TGGAAATTGT

Locomotor function (experiments two and three)

To evaluate the effect of treatment of IL-19 on recovery of locomotor function, the BMS scoring was applied. As expected, SCI led to complete paralysis of hindlimbs (BMS score 0) 24 h after injury with slow recovery of locomotor function during the following 2 weeks. In experiment two, treatment with exogenous IL-19 promoted the recovery of locomotor function in a dose-dependent manner (Figure 2A). In experiment three, IL-19 blocking antibody treatment abolished the effects of exogenous IL-19 on functional recovery in SCI mice (Figure 2B).

Loss of motor neurons and microglial and glial activation (experiment three)

To investigate the effect of IL-19 treatment on loss of motor neurons and microglial and glial action, immunofluorescence staining, RT-PCR and Western blotting analysis were applied. Treatment of SCI mice with IL-19 increased the number of NeuN-positive cells (Figure 3A, D) and reduced staining intensity of GFAP (Figure 3B, D) and IBA1-positive cells (Figure 3C, D). RT-PCR and Western blotting analysis results revealed that administration of exogenous IL-19 up-regulated the mRNA and protein levels of NeuN and down-regulated the mRNA (Figure 3E) and protein (Figure 3F) levels of GFAP and IBA1 in injured spinal cords. Exogenous IL-19 also protected against loss of

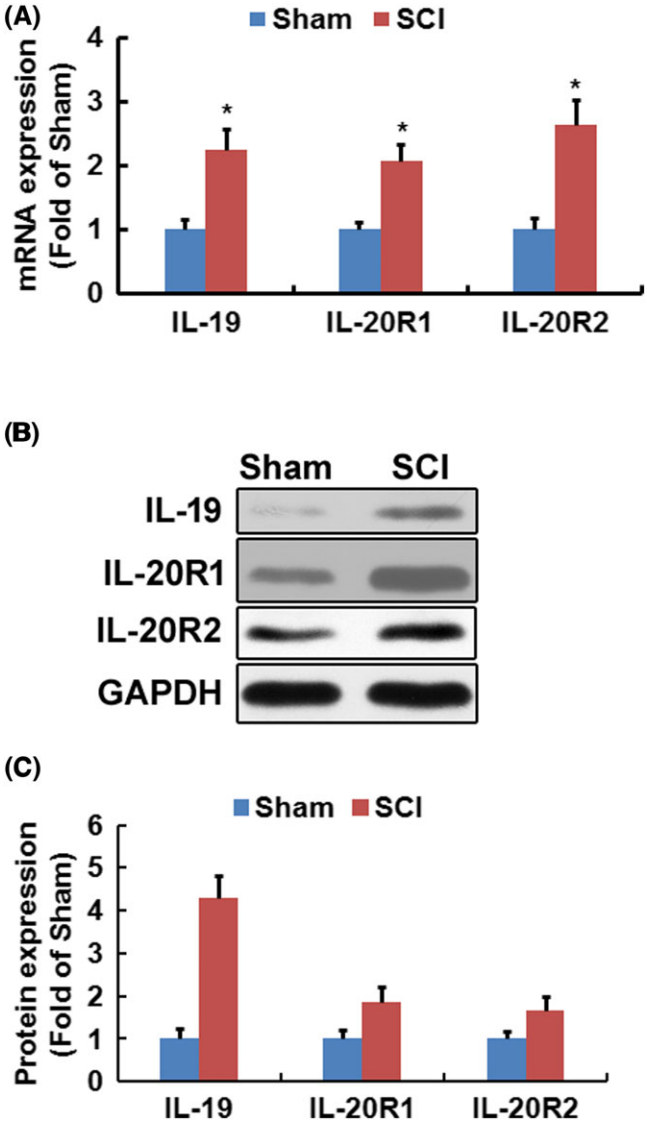

Figure 1

Spinal cord trauma up-regulated expression of IL-19 and its receptor in spinal cord. Gene expression (A) of IL-19, IL-20R1 and IL-20R2 was measured by quantitative real-time PCR (n = 8). In (B), the results from Western blotting and the corresponding quantification (n = 3) for IL-19, IL-20R1 and IL-20R2 were shown. Data shown are the means ± SD. *P < 0.05, significantly different from the sham-operated mice.

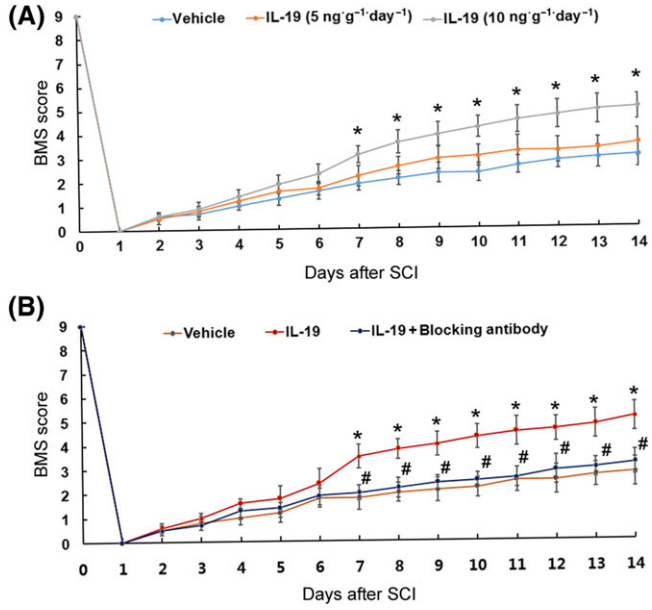

Figure 2

Mice were exposed to spinal cord trauma and treated i.p. with IL-19 (5 and 10 ng·g^{-1} day^{-1}) or vehicle (A). Mice were randomly divided into three groups as follows: (i) SCI mice treated with vehicle; (ii) SCI mice treated with IL-19 (10 ng·g^{-1} ·day^{-1}, i.p.); and (iii) SCI mice treated with IL-19 (10 ng·g^{-1} ·day^{-1}, i.p.) and IL-19 blocking antibody (10 mg·kg^{-1}·day^{-1}, s.c.) (B). The time courses of locomotor recovery evaluated by the 9-point BMS scoring after SCI are shown. Data shown are the means ± SD. n = 7 in each group; *P < 0.05, significantly different from the vehicle-treated group; #P < 0.05, significantly different from the IL-19-treated group.

motor neurons and microglial and glial activation following SCI, which was abolished by treatment with IL-19 blocking antibody.

Immune modulation (experiment three)

As shown in the results of immunofluorescence staining and RT-PCR, treatment of SCI mice with IL-19 reduced the staining intensity of CD68-positive cells (Figure 4A, B) and mRNA expression (Figure 4C) of CD68, indicating that IL-19 treatment reduced macrophage accumulation in SCI lesions. Furthermore, treatment of SCI mice with IL-19 reduced protein levels of TNF-α (Figure 4D) and CCL2 (Figure 4E) in the injured region. Our results suggested that IL-19 treatment suppressed inflammation following SCI, which was abolished by IL-19 blocking antibody.

The immune status in whole spleen of mice of two groups was evaluated by measurement of the expression of Th1 and Th2 markers by RT-PCR. The spleens were rapidly removed from mice at the end of our study. Whole spleen lysates from IL-19-treated mice had significantly lower mRNA expression of the Th1 markers T-bet (Figure 4F) and higher mRNA expression of GATA-3 (Figure 4G).

Treatment with IL-19 reduced mRNA expression of **IFN-γ** (Figure 4H, a Th1 marker), IL-12 (Figure 4I), **inducible NOS** (M1 markers, Figure 4J) and enhanced mRNA expression of **arginase-1 (Arg1)** (Figure 4K), Ym1 (Figure 4M) and CD206 (Figure 4N, M2 markers) in the injured spinal cord. In addition, whole spleen lysates from IL-19-treated mice had significantly lower mRNA expression of IFN-γ and IL-12 and higher mRNA expression of Arg1, Ym1 and CD206. Our results suggested that IL-19 treatment promoted a shift towards a Th2 response following SCI, which was abolished by treatment with IL-19 blocking antibody.

Angiogenesis (experiment three)

To evaluate the effect of treatment of IL-19 on angiogenesis following SCI, expression of VEGF and PECAM-1 was

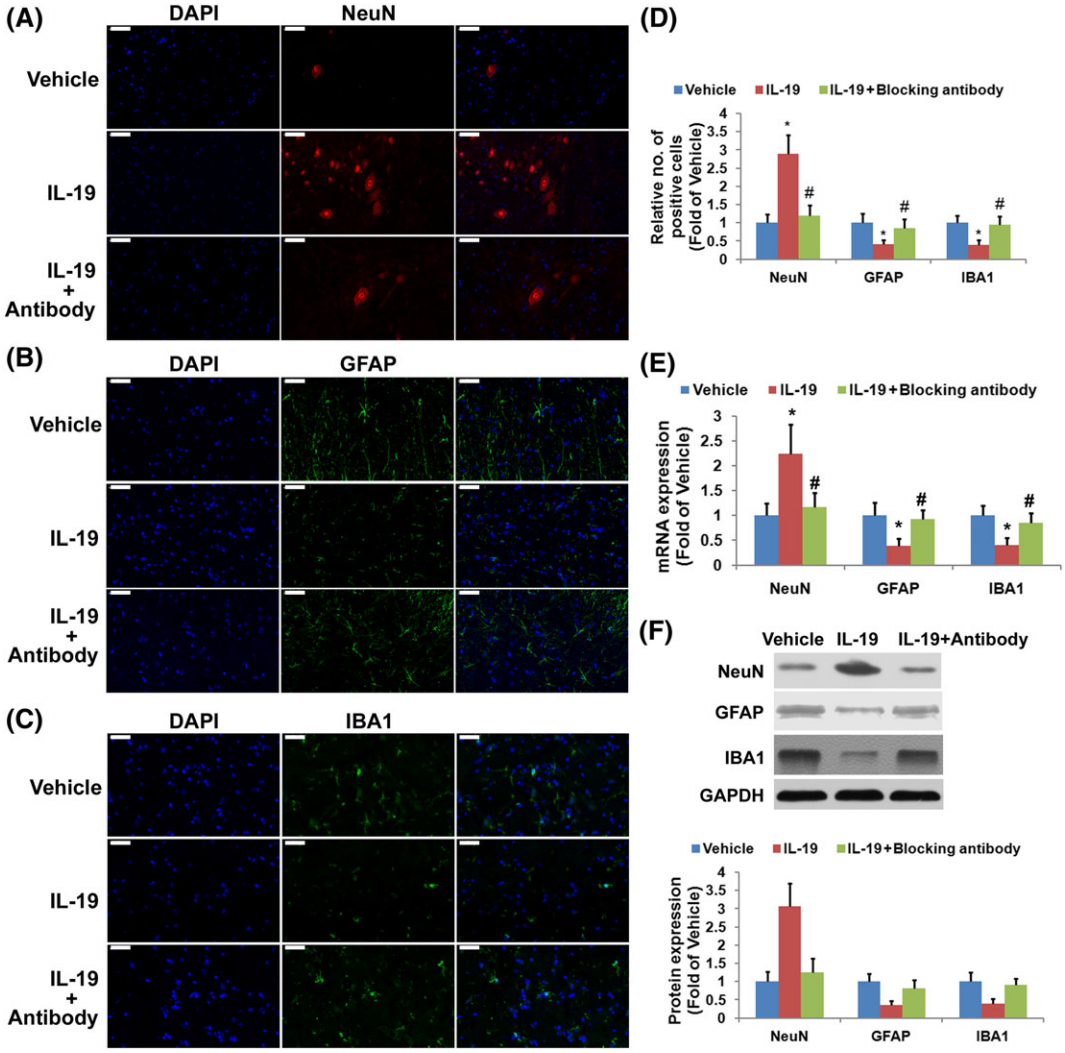

Figure 3

Effects of treatment with IL-19 (10 ng·g^{-1}·day^{-1}) and IL-19 blocking antibody (10 mg·kg^{-1}·day^{-1}) on loss of motor neurons and microglial and glial activation in mice exposed to SCI. Sections (2 mm rostral to the epicentre, scale bar = 50 μm) were immuno-stained with antibodies recognizing NeuN (A), activated glial (GFAP, B) and microglia (IBA1, C) and the corresponding quantification (D). The mRNA (E) and protein (F) expressions of NeuN, GFAP and IBA1 were determined by quantitative real-time PCR and Western blotting respectively. Data shown are the means ± SD; $n = 7$ in each group. *$P < 0.05$, significantly different from the vehicle-treated group; #$P < 0.05$, significantly different from the IL-19-treated group.

determined. The predominant isoforms of VEGF in the CNS of mice were $VEGF_{120}$, $VEGF_{164}$ and $VEGF_{188}$ (Figley *et al.*, 2014). It was found that treatment of SCI mice with IL-19 up-regulated mRNA expression of $VEGF_{120}$ and $VEGF_{164}$ (Figure 5A) in the injured spinal cord but had no significant effect on mRNA expression of $VEGF_{188}$. Furthermore, Western blotting analysis revealed that treatment of SCI mice with IL-19 enhanced protein levels of PECAM-1 (Figure 5B) and VEGF-A (Figure 5C) in the injured spinal cord. Our results suggested that IL-19 promoted angiogenesis through up-regulating VEGF expression following SCI, which was abolished by treatment with IL-19 blocking antibody.

Oxidative stress (experiment three)

Western blotting and RT-PCR analysis revealed that treatment of SCI mice with IL-19 up-regulated protein (Figure 6A) and mRNA (Figure 6B) expression of HO-1 in the injured spinal cord. Furthermore, treatment of SCI mice with IL-19 reduced levels of MDA (Figure 6C, marker of lipid peroxidation) in the injured region. Our results suggested that IL-19 decreased oxidative stress through up-regulating HO-1 expression following SCI, which was abolished by treatment with IL-19 blocking antibody.

Effect of IL-19 deficiency on locomotor function following SCI (experiment four)

To further confirm the role of IL-19 in the recovery from SCI, locomotor function was examined directly in IL-19 (−/−) mice and wild-type mice. All the mice had a BMS score of 9 pre-injury and a score of 0 1 day after surgery, with bilateral hindlimb paralysis. However, in mice with IL-19 deleted,

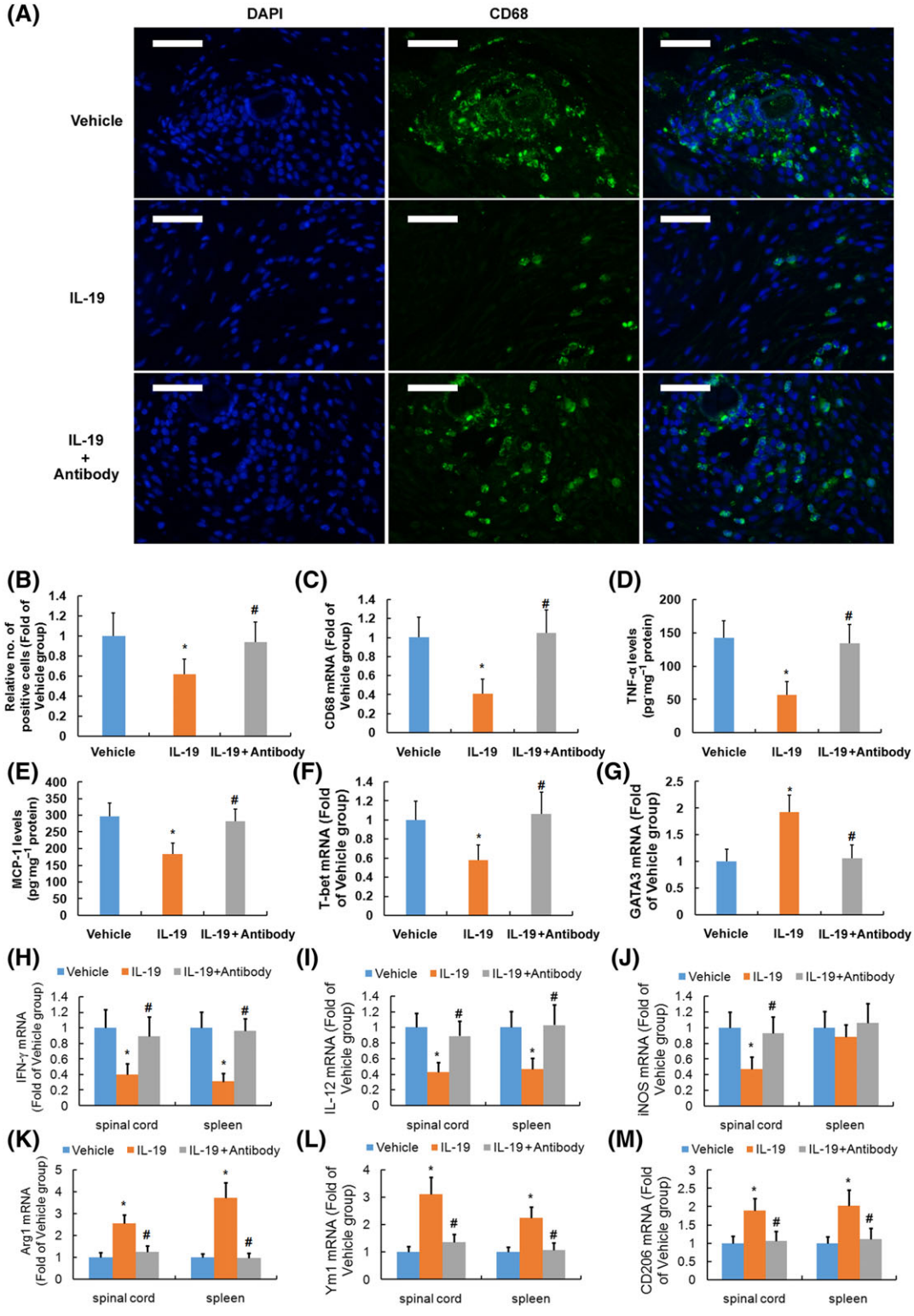

Figure 4

Immune modulation of treatment with IL-19 (10 ng·g^{-1}·day^{-1}) and IL-19 blocking antibody (10 mg·kg^{-1}·day^{-1}) in mice with SCI. Representative micrographs (A) and corresponding quantification (B) of lumbar spinal cord sections (2 mm rostral to epicentre, scale bar = 50 μm) stained for immunofluorescence using antibody recognizing CD68 are shown. Graphs show the mRNA levels of CD68 (C) and protein levels of TNF-α (D) and CCL2 (E) in spinal cord, mRNA levels of T-bet (F) and GATA-3 (G) in spleen, and mRNA levels of IFN-γ (H), IL-12 (I), inducible NOS (iNOS) (J), Arg1 (K), Ym1 (M) and CD206 (N) in spinal cord and spleen of mice. Data shown are the means ± SD; $n = 7$ in each group. *$P < 0.05$, significantly different from the vehicle-treated group; #$P < 0.05$, significantly different from the IL-19-treated group.

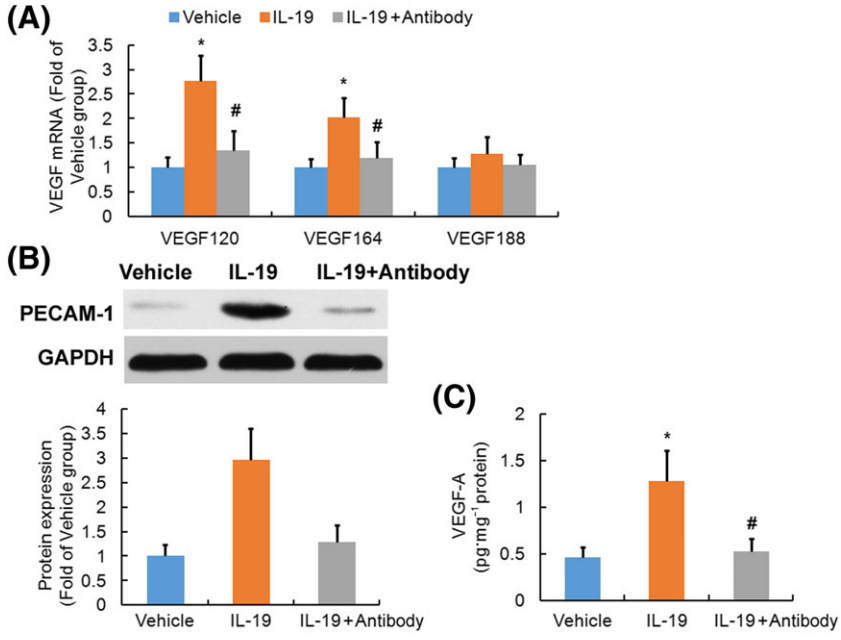

Figure 5

Effects of treatment with IL-19 (10 ng·g^{-1}·day^{-1}) and IL-19 blocking antibody (10 mg·kg^{-1}·day^{-1}) on angiogenesis in spinal cord of mice exposed to SCI. Graphs show the mRNA levels (n = 7) of three isoforms of VEGF (A, $VEGF_{120}$, $VEGF_{164}$, and $VEGF_{188}$) in the injured spinal cords. In (B), Western blotting results and the corresponding quantification (B, n = 3) of PECAM-1 are shown. VEGF-A protein levels (C, n = 7) in spinal cord were determined by ELISA. Data shown are the means ± SD. *$P < 0.05$, significantly different from the vehicle-treated group; #$P < 0.05$, significantly different from the IL-19-treated group.

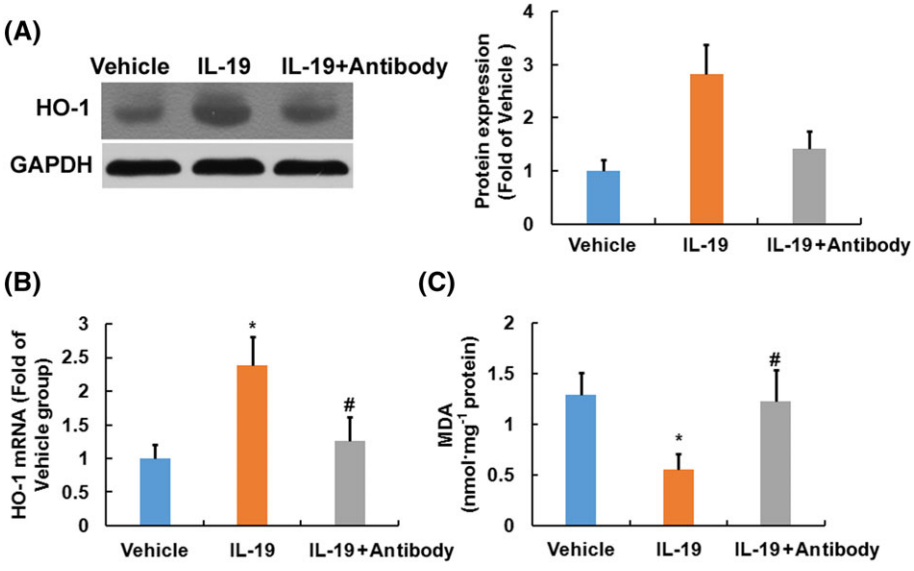

Figure 6

Effects of treatment with IL-19 (10 ng·g^{-1}·day^{-1}) and IL-19 blocking antibody (10 mg·kg^{-1}·day^{-1}) on oxidative stress in spinal cord of mice exposed to SCI. In (A), Western blotting results and the corresponding quantification (n = 3) of HO-1 are shown. Graphs show the mRNA levels (n = 7) of HO-1 (B) and the levels of MDA (C) in the injured spinal cords. Data shown are the means ± SD. *$P < 0.05$, significantly different from the vehicle-treated group; #$P < 0.05$, significantly different from the IL-19-treated group.

the recovery of locomotor function following SCI was clearly delayed (Figure 7).

Discussion

In the present study, we provided evidence that IL-19 signalling was up-regulated following SCI and treatment with exogenous IL-19 improved the recovery of locomotor function in SCI mice. Deletion of IL-19 delayed the recovery of locomotor function following SCI, which further confirmed the protective role of IL-19 against spinal cord trauma. In the current study, our results suggested that IL-19 promoted a shift towards a Th2 response, decreased oxidative stress and enhanced angiogenesis, which might contribute to the recovery of motor function, after IL-19 treatment for SCI. Furthermore, treatment with an antibody that blocked the effects of IL-19, abolished the effects of exogenous IL-19 on immune cell polarization, angiogenesis and anti-oxidative response.

The local inflammatory micro-environment mediated by activated microglia and astrocytes and macrophages derived from infiltrating monocytes contributes greatly to the progression of secondary injury following SCI (Hayakawa *et al.*, 2014; Plemel *et al.*, 2014). Exposure of macrophages to Th1 cytokines, such as IFN-γ and TNF-α, resulted in their polarization to the M1 subpopulation (the classical activated pro-inflammatory macrophages), which was detrimental in SCI (Sharma *et al.*, 2003; Kigerl *et al.*, 2009). By contrast, the 'alternatively activated anti-inflammatory' M2 macrophages, induced by Th2 cytokines such as IL-4, IL-10 and IL-13, promoted axonal regeneration after CNS injury (Ma *et al.*, 2015; Francos-Quijorna *et al.*, 2016). In the injured spinal cord, the polarization of microglia/macrophages was M1 predominant and lasted longer (Wang *et al.*, 2015). IL-19 was reported to be anti-inflammatory because in T-lymphocytes, it promoted the Th2, rather than the Th1 response (Gallagher *et al.*, 2004; Gallagher, 2010). In experimental models of atherosclerosis, splenocytes from IL-19-treated mice showed immune cell Th2 polarization, and plaque characterization showed an enrichment in markers of M2 macrophages (Ellison *et al.*, 2013; Gabunia *et al.*, 2016). When compared with vehicle-injected controls, IL-19-treated mice had increased expression of M2 markers (Gabunia and Autieri, 2015; Richards *et al.*, 2015). In the current study, treatment of SCI mice with IL-19 promoted Th2 cytokine synthesis and led to the polarization of spinal macrophages/microglial cells towards an M2 phenotype, ultimately shifting the immune imbalance towards anti-inflammation that was conducive to the rescue of residual myelin and neurons and preservation of neuronal function.

Angiogenesis after SCI promoted endogenous repair and supported neural regeneration (Figley *et al.*, 2014; Yu *et al.*, 2016). In the aortic ring model of angiogenesis (Kako *et al.*, 2016) and the hindlimb ischaemia induced by femoral artery ligation (Gabunia and Autieri, 2015; Richards *et al.*, 2015), IL-19 increased angiogenesis. In the current study, treatment of SCI mice with IL-19 increased expression of PECAM-1, which suggested that IL-19 promoted angiogenesis in the injured spinal cord. Macrophages polarized towards an M2 phenotype expressed a considerable number of angiogenic growth factors and had a higher angiogenic potential compared with other subsets (Jetten *et al.*, 2014), which could partly explain the angiogenic potential of IL-19. Accumulating evidence revealed that VEGF-A, known to promote the proliferation of endothelial cells and initiate angiogenesis, was a primary driver of neovascularization and had neuroprotective effects (Shweiki *et al.*, 1992). In bone marrow-derived macrophages, IL-19 treatment induced expression of VEGF-A (Gabunia and Autieri, 2015; Richards *et al.*, 2015). In the current study, treatment with IL-19 enhanced mRNA expression of $VEGF_{120}$ and $VEGF_{164}$, and protein levels of VEGF-A. Additionally, IL-19 expression and activity were not restricted to leukocytes as IL-19 was also expressed in angiogenic tissue and has potent pro-angiogenic effects on many human endothelial cell types, including those from umbilical vein, coronary artery and the microvasculature (Jain *et al.*, 2011).

In the current study, treatment with exogenous IL-19 up-regulated expression of HO-1 in the injured spinal cord. This enzyme is rate limiting in the conversion of the pro-oxidant haem to equimolar quantities of the potent antioxidant biliverdin, which was rapidly converted to bilirubin, as well as carbon monoxide (Maines, 2000). HO-1 was expressed in the vascular compartment and in recruited neutrophils after SCI, and HO-1 induction attenuated neutrophil infiltration and microglial activation and decreased oxidative stress in the injured spinal cord (Hervera *et al.*, 2012; Lin *et al.*, 2016). IL-19 induced expression of HO-1 and protected

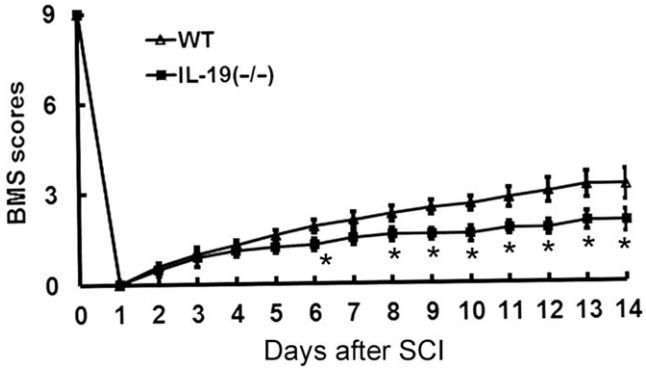

Figure 7

Effects of knockout of the IL-19 gene on locomotor function in mice exposed to spinal cord trauma. The time courses of locomotor recovery evaluated by the 9-point BMS scoring after SCI are shown. Data shown are the means ± SD; $n = 6$ in each group. *$P < 0.05$, significantly different from the wild-type mice.

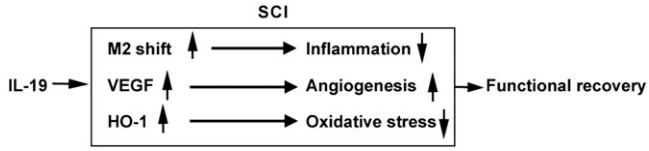

Figure 8

A diagram illustrating the effects of IL-19 in secondary injuries and functional recovery after SCI.

cultured vascular smooth muscle cells from ROS-induced and starvation-induced apoptosis (Gabunia *et al*., 2012). In the current study, IL-19 decreased oxidative stress, as shown by reduced lipid peroxidation, which could contribute to up-regulation of HO-1 and the reduced infiltration of macrophages in injured spinal cord.

In conclusion, IL-19 treatment reduced secondary injuries and improved locomotor functional recovery after contusion SCI, through many different mechanisms, including immune cell polarization, angiogenesis and anti-oxidative response (Figure 8). Thus, IL-19 may be envisaged as a therapeutic strategy for patients with acute contusion SCI, but more work in animals and patients is required.

Author contributions

Conception and design of the experiments were carried out by J.G., H.W., L.L. and S.H. Collection, analysis and interpretation of data were performed by J.G., H.W., L.L., Y.Y. and X.S. Drafting the article was performed by J.G. and S.H.

Conflict of interest

The authors declare no conflicts of interest.

Declaration of transparency and scientific rigour

This Declaration acknowledges that this paper adheres to the principles for transparent reporting and scientific rigour of preclinical research recommended by funding agencies, publishers and other organisations engaged with supporting research.

References

Alexander SP, Fabbro D, Kelly E, Marrion NV, Peters JA, Faccenda E *et al*. (2017a). The Concise Guide to PHARMACOLOGY 2017/18: Catalytic receptors. Br J Pharmacol 174 (Suppl 1): S225–S271.

Alexander SP, Fabbro D, Kelly E, Marrion NV, Peters JA, Faccenda E *et al*. (2017b). The Concise Guide to PHARMACOLOGY 2017/18: Enzymes. Br J Pharmacol 174 (Suppl 1): S272–S359.

Basso DM, Fisher LC, Anderson AJ, Jakeman LB, McTigue DM, Popovich PG (2006). Basso Mouse Scale for locomotion detects differences in recovery after spinal cord injury in five common mouse strains. J Neurotrauma 23: 635–659.

Curtis MJ, Bond RA, Spina D, Ahluwalia A, Alexander SP, Giembycz MA *et al*. (2015). Experimental design and analysis and their reporting: new guidance for publication in BJP. Br J Pharmacol 172: 3461–3471.

Dumoutier L, Leemans C, Lejeune D, Kotenko SV, Renauld JC (2001). Cutting edge: STAT activation by IL-19, IL-20 and mda-7 through IL-20 receptor complexes of two types. J Immunol 167: 3545–3549.

Ellison S, Gabunia K, Kelemen SE, England RN, Scalia R, Richards JM *et al*. (2013). Attenuation of experimental atherosclerosis by interleukin-19. Arterioscler Thromb Vasc Biol 33: 2316–2324.

Ellison S, Gabunia K, Richards JM, Kelemen SE, England RN, Rudic D *et al*. (2014). IL-19 reduces ligation-mediated neointimal hyperplasia by reducing vascular smooth muscle cell activation. Am J Pathol 184: 2134–2143.

Figley SA, Liu Y, Karadimas SK, Satkunendrarajah K, Fettes P, Spratt SK *et al*. (2014). Delayed administration of a bio-engineered zinc-finger VEGF-A gene therapy is neuroprotective and attenuates allodynia following traumatic spinal cord injury. PLoS One 9: e96137.

Francos-Quijorna I, Amo-Aparicio J, Martinez-Muriana A, López-Vales R (2016). IL-4 drives microglia and macrophages toward a phenotype conducive for tissue repair and functional recovery after spinal cord injury. Glia 64: 2079–2092.

Gabunia K, Ellison S, Kelemen S, Kako F, Cornwell WD, Rogers TJ *et al*. (2016). IL-19 halts progression of atherosclerotic plaque, polarizes, and increases cholesterol uptake and efflux in macrophages. Am J Pathol 186: 1361–1374.

Gabunia K, Autieri MV (2015). Interleukin-19 can enhance angiogenesis by macrophage polarization. Macrophage (Houst) 2: e562.

Gabunia K, Ellison SP, Singh H, Datta P, Kelemen SE, Rizzo V *et al*. (2012). Interleukin-19 (IL-19) induces heme oxygenase-1 (HO-1) expression and decreases reactive oxygen species in human vascular smooth muscle cells. J BiolChem 287: 2477–2784.

Gallagher G, Dickensheets H, Eskdale J, Izotova LS, Mirochnitchenko OV, Peat JD *et al*. (2000). Cloning, expression and initial characterization of interleukin-19 (IL-19), a novel homologue of human interleukin-10 (IL-10). Genes Immun 1: 442–450.

Gallagher G, Eskdale J, Jordan W, Peat J, Campbell J, Boniotto M *et al*. (2004). Human interleukin-19 and its receptor: a potential role in the induction of Th2 responses. IntImmunopharmacol 4: 615–626.

Gallagher G (2010). Interleukin-19: multiple roles in immune regulation and disease. Cytokine Growth Factor Rev 21: 345–352.

Harding SD, Sharman JL, Faccenda E, Southan C, Pawson AJ, Ireland S *et al*. (2018). The IUPHAR/BPS Guide to PHARMACOLOGY in 2018: updates and expansion to encompass the new guide to IMMUNOPHARMACOLOGY. Nucl Acids Res 46: D1091–D1106.

Hayakawa K, Okazaki R, Morioka K, Nakamura K, Tanaka S, Ogata T (2014). Lipopolysaccharide preconditioning facilitates M2 activation of resident microglia after spinal cord injury. J Neurosci Res 92: 1647–1658.

Hervera A, Leánez S, Negrete R, Motterlini R, Pol O (2012). Carbon monoxide reduces neuropathic pain and spinal microglial activation by inhibiting nitric oxide synthesis in mice. PLoS One 7: e43693.

Horiuchi H, Parajuli B, Wang Y, Azuma YT, Mizuno T, Takeuchi H *et al*. (2015). Interleukin-19 acts as a negative autocrine regulator of activated microglia. PLoS One 10: e0118640.

Hsu YH, Hsieh PP, Chang MS (2012). Interleukin-19 blockade attenuates collagen-induced arthritis in rats. Rheumatology (Oxford) 51: 434–442.

Jain S, Gabunia K, Kelemen SE, Panetti TS, Autieri MV (2011). The anti-inflammatory cytokine interleukin 19 is expressed by and angiogenic for human endothelial cells. Arterioscler Thromb Vasc Biol 31: 167–175.

Jakeman LB, Guan Z, Wei P, Ponnappan R, Dzwonczyk R, Popovich PG *et al*. (2000). Traumatic spinal cord injury produced by controlled contusion in mouse. J Neurotrauma 17: 299–319.

Jetten N, Verbruggen S, Gijbels MJ, Post MJ, De Winther MP, Donners MM (2014). Anti-inflammatory M2, but not pro-inflammatory M1 macrophages promote angiogenesis in vivo. Angiogenesis 17: 109–118.

Jia Z, Zhu H, Li J, Wang X, Misra H, Li Y (2012). Oxidative stress in spinal cord injury and antioxidant-based intervention. Spinal Cord 50: 264–274.

Kako F, Gabunia K, Ray M, Kelemen SE, England RN, Kako B *et al*. (2016). Interleukin-19 induces angiogenesis in the absence of hypoxia by direct and indirect immune mechanisms. Am J Physiol Cell Physiol 310: C931–C941.

Kigerl KA, Gensel JC, Ankeny DP, Alexander JK, Donnelly DJ, Popovich PG (2009). Identification of two distinct macrophage subsets with divergent effects causing either neurotoxicity or regeneration in the injured mouse spinal cord. J Neurosci 29: 13435–13444.

Kilkenny C, Browne W, Cuthill IC, Emerson M, Altman DG (2010). NC3Rs reporting guidelines working group. Br J Pharmacol 160: 1577–1579.

Lin WP, Xiong GP, Lin Q, Chen XW, Zhang LQ, Shi JX *et al*. (2016). Heme oxygenase-1 promotes neuron survival through down-regulation of neuronal NLRP1 expression after spinal cord injury. J Neuroinflammation 13: 52.

Ma SF, Chen YJ, Zhang JX, Shen L, Wang R, Zhou JS *et al*. (2015). Adoptive transfer of M2 macrophages promotes locomotor recovery in adult rats after spinal cord injury. Brain Behav Immun 45: 157–170.

Maines MD (2000). The heme oxygenase system and its functions in the brain. Cell MolBiol (Noisy-le-grand) 46: 573–585.

Matsuo Y, Azuma YT, Kuwamura M, Kuramoto N, Nishiyama K, Yoshida N *et al*. (2015). Interleukin 19 reduces inflammation in chemically induced experimental colitis. IntImmunopharmacol 29: 468–475.

McDonald JW, Sadowsky C (2002). Spinal cord injury. Lancet 359: 417–425.

McGrath JC, Lilley E (2015). Implementing guidelines on reporting research using animals (ARRIVE etc.): new requirements for publication in BJP. Br J Pharmacol 172: 3189–3193.

Oyinbo CA (2011). Secondary injury mechanisms in traumatic spinal cord injury: a nugget of this multiply cascade. Acta Neurobiol Exp (Wars) 71: 281–299.

Plemel JR, Wee Yong V, Stirling DP (2014). Immune modulatory therapies for spinal cord injury – past, present and future. Exp Neurol 258: 91–104.

Ren Y, Young W (2013). Managing inflammation after spinal cord injury through manipulation of macrophage function. Neural Plast 2013: 945034.

Richards J, Gabunia K, Kelemen SE, Kako F, Choi ET, Autieri MV (2015). Interleukin-19 increases angiogenesis in ischemic hind limbs by direct effects on both endothelial cells and macrophage polarization. J Mol Cell Cardiol 79: 21–31.

Sabat R, Wallace E, Endesfelder S, Wolk K (2007). IL-19 and IL-20: two novel cytokines with importance in inflammatory diseases. Expert Opin Ther Targets 11: 601–612.

Sharma HS, Winkler T, Stålberg E, Gordh T, Alm P, Westman J (2003). Topical application of TNF-alpha antiserum attenuates spinal cord trauma induced edema formation, microvascular permeability disturbances and cell injury in the rat. Acta Neurochir Suppl 86: 407–413.

Shweiki D, Itin A, Soffer D, Keshet E (1992). Vascular endothelial growth factor induced by hypoxia may mediate hypoxia-initiated angiogenesis. Nature 359: 843–845.

Wang X, Cao K, Sun X, Chen Y, Duan Z, Sun L *et al*. (2015). Macrophages in spinal cord injury: phenotypic and functional change from exposure to myelin debris. Glia 63: 635–651.

Xie W, Fang L, Gan S, Xuan H (2016). Interleukin-19 alleviates brain injury by anti-inflammatory effects in a mice model of focal cerebral ischemia. Brain Res 1650: 172–177.

Yu S, Yao S, Wen Y, Wang Y, Wang H, Xu Q (2016). Angiogenic microspheres promote neural regeneration and motor function recovery after spinal cord injury in rats. Sci Rep 6: 33428.